CELL STRUCTURE AND FUNCTION 41: 145–152 (2016)

Pericentric H3K9me3 Formation by HP1 Interaction-defective Histone Methyltransferase Suv39h1

Daisuke Muramatsu[1,2], Hiroshi Kimura[3], Kaoru Kotoshiba[2], Makoto Tachibana[1,4], and Yoichi Shinkai[2,5]*

[1]*Graduate School of Biostudies, Kyoto University, 53 Shogoin, Kawara-cho, Sakyo-ku, Kyoto 606-8507, Japan,* [2]*Cellular Memory Laboratory, RIKEN, Wako, Saitama 351-0198, Japan,* [3]*Graduate School of Bioscience and Biotechnology, Tokyo Institute of Technology, 4259 Nagatsuta, Midori-ku, Yokohama 226-8501, Japan,* [4]*Institute for Virus Research, Kyoto University, 53 Shogoin, Kawara-cho, Sakyo-ku, Kyoto 606-8507, Japan,* [5]*JST, CREST, Wako, Saitama 351-0198, Japan*

ABSTRACT. **Pericentric regions form epigenetically organized, silent heterochromatin structures that accumulate histone H3 lysine 9 tri-methylation (H3K9me3) and heterochromatin protein 1 (HP1), a methylated H3K9-binding protein. At pericentric regions, Suv39h is the major enzyme that generates H3K9me3. Suv39h also interacts directly with HP1. However, the importance of HP1 interaction for Suv39h-mediated H3K9me3 formation at the pericentromere is not well characterized. To address this question, we introduced HP1 binding-defective, N-terminally truncated mouse Suv39h1 (ΔN) into *Suv39h*-deficient cells. Pericentric H3K9me3-positive cells were not detected by endogenous-level expression of ΔN. Notably, ΔN could induce pericentric accumulation of H3K9me3 as wild type Suv39h1 did if it was overexpressed. These findings demonstrate that the N-terminal region of Suv39h1, presumably via HP1–Suv39h1 interaction, is required for Suv39h1-mediated pericentric H3K9me3 formation, but can be overridden if Suv39h1 is overproduced, indicating that Suv39h1-mediated heterochromatin formation is controlled by multiple modules, including HP1.**

Key words: H3K9 methylation, HP1, major satellite repeats, Suv39h

Introduction

Chromatin exists in two forms: euchromatin and heterochromatin (Allis *et al.*, 2007). Euchromatin is a loosely packed form of chromatin that has a high gene concentration and is often undergoing active transcription. In contrast, heterochromatin is tightly packed and in a transcriptionally repressed state. The pericentromere is a heterochromatic domain that provides a structural scaffold for centromere formation and plays a crucial role in genome stability (Allshire and Karpen, 2008). In mice, pericentric heterochromatin consists of AT-rich sequences of extremely long tandem arrays of major satellite repeats (Vissel and Choo, 1989). Therefore, the fluorochrome DAPI, which preferentially intercalates with AT-rich repeat sequences, can label mouse pericentromere heterochromatin as a DAPI-dense domain.

*To whom correspondence should be addressed: Yoichi Shinkai, Cellular Memory Laboratory, RIKEN, 2-1 Hirosawa, Wako-city, Saitama 351-0198, Japan.
Tel: +81–048–467–9370, Fax: +81–3–048–462–4670
E-mail: yshinkai@riken.jp

In addition to repetitive sequences, the pericentric heterochromatin has a distinct combination of epigenetic marks such as histone H3 lysine 9 tri-methylation (H3K9me3), H4K20me3, and DNA methylation (Allis *et al.*, 2007; Black and Whetstine, 2011). Suv39h/KMT1A is the principal enzyme responsible for H3K9me3 of pericentromere heterochromatin in mammals, and is evolutionarily conserved. Since Suv39h also indirectly regulates H4K20me3 and DNA methylation, the expression of these epigenetic marks are also decreased or lost in the pericentromere of *Suv39h*-deficient cells (Lehnertz *et al.*, 2003; Schotta *et al.*, 2004). Thus, Suv39h is one of the master regulators of epigenetically organized heterochromatin.

One important role of these epigenetic modifications is recruitment of transcriptionally silent effector molecules to specific chromatin loci (Kouzarides and Berger, 2007; Taverna *et al.*, 2007). Heterochromatin Protein 1 (HP1) is an effector molecule that was originally discovered in *Drosophila* as a dominant suppressor of position-effect variegation (Eissenberg *et al.*, 1990). Similar to Suv39h, the HP1 family is evolutionarily conserved, with members in fungi, plants, and animals, and has multiple isoforms

within the same species (Zeng *et al.*, 2010). The amino-terminal chromodomain (CD) has high affinity for methylated H3K9 (with the highest affinity for H3K9me3) and causes HP1 to be tethered to heterochromatin (Bannister *et al.*, 2001; Lachner *et al.*, 2001). This recruitment system is also highly conserved in different species. This recruitment system is also highly conserved in different species. For example, in fission yeast, the HP1 homolog Swi6 is crucial for the Suv39h homolog Clr4 accumulation and Clr4-mediated H3K9 methylation of heterochromatin (Hall *et al.*, 2002). Furthermore, HP1 homologs can physically interact with Suv39h homologs in various species. Sequential cycles of Swi6 binding and Clr4 recruitment/deposition of H3K9me have been proposed to explain the interdependent regulation of Clr4- and Swi6-mediated silent heterochromatin formation (Grewal and Elgin, 2002).

A similar model has been proposed for Suv39h- and HP1-mediated heterochromatin formation in mammals (Bannister *et al.*, 2001; Lachner *et al.*, 2001). However, whether Suv39h-HP1 interaction is crucial for Suv39h-mediated heterochromatin formation has not been experimentally validated, and will be addressed in this study.

Materials and Methods

Cells and culture conditions

Eco-Pack 2-293 (Clontech) and HEK293T cells were cultured in Dulbecco's modified Eagle's medium (DMEM) with high glucose (D6429, Sigma) supplemented with 10% fetal calf serum (FCS). Wild-type and *Suv39h* DKO ES cells (Lehnertz *et al.*, 2003) were grown in DMEM with high glucose supplemented with 15% FCS, 0.1 mM β-mercaptoethanol, leukemia-inhibiting factor, and 1× non-essential amino acids. *Suv39h* DKO iMEFs (Lachner *et al.*, 2001) were cultured in DMEM with high glucose supplemented with 10% FCS, 0.1 mM β-mercaptoethanol, and 1× non-essential amino acids.

Plasmids

DNA fragments encoding Flag-tagged wild type (WT) Suv39h1 (Flag-Suv39h1 WT) and N-terminal-truncated mutant Suv39h1$^{(\Delta 1–41)}$ (ΔN) were subcloned into the pPBCAGGS-IRESpuro vector (Ohtsuka *et al.*, 2012) used to establish *Suv39h* DKO ES cells stably expressing Flag-Suv39h1 or ΔN, and the pMCs-IRES-GFP vector (Cell Biolabs, Inc.) for producing retroviruses for expression of Flag-Suv39h1 WT or ΔN in *Suv39h* DKO iMEFs. DNA fragments encoding Myc-tagged mouse HP1α, HP1β and HP1γ were cloned into the pcDNA3.1 vector.

Antibodies

Antibodies used for western blotting, immunoprecipitation (IP), and immunofluorescence analyses were anti-H3K9me3 (2F3, (Chandra *et al.*, 2012)), anti-HP1β (BMP002, MBL), anti-Flag M2 (F3165, Sigma), anti-Myc (9E10), anti-Suv39h1 (D11B6, Cell Signaling), HRP-conjugated anti-mouse Ig (RKL, 18-8817-31) or anti-rabbit IgG (H+L) (170-6515, BioRad,), and Alexa Fluor® 488, 546, or 647 fluorophore-conjugated anti-mouse or anti-rabbit IgG (Thermo Fisher Scientific).

Western blot analysis

For protein expression analysis, total cell lysates were sonicated in 1× SDS sample buffer, separated by SDS-PAGE and transferred to nitrocellulose or PVDF membrane. Before blocking and primary antibody hybridization, the transferred membrane was stained with Ponceau S.

Protein co-immunoprecipitation

Forty-eight hours after transfection, HEK293 T cells were incubated in PBS containing 5 mM DTBP at 4°C for 1 h. Whole cell lysate was obtained using lysis buffer (150 mM NaCl, 50 mM Tris-HCl pH 7.5, 0.3% digitonin, 20 mM *N*-ethylmaleimide) after quenching for 10 min at 4°C using PBS buffer with 150 mM glycine. The lysate was then used for either Flag-IP or Myc-IP. For Flag-IP, the lysate was incubated with anti-Flag antibody affinity gel (A2220-10ML, Sigma) for 2 h at 4°C. The immune complex was washed three times with washing buffer (150 mM NaCl, 50 mM Tris-HCl pH 7.5, 0.1% digitonin) before precipitated proteins were eluted by an excess amount of 3× FLAG peptide (F4799, Sigma). For Myc-IP, the lysate was incubated with anti-Myc antibody for 2 h at 4°C. The immune complex was captured using Protein G sepharose (17-0618-02, GE healthcare) and washed with washing buffer.

Establishment of Suv39h DKO ES cells stably expressing Flag-Suv39h1 WT or ΔN

To generate *Suv39h* DKO ES cells stably expressing Suv39h1 WT or ΔN, the pPBCAGGS-IRESpuro vector containing Flag-Suv39h1 WT or -ΔN, and a transposase expression vector, pCAGGS-PBase, were co-transfected into *Suv39h* DKO ES cells by lipofection with Lipofectamine® 2000 (Thermo Fisher Scientific). Stably expressing cells were selected in ES medium containing 1 μg ml^{-1}puromycin.

Establishment of Suv39h DKO iMEF cells stably expressing Flag-Suv39h1 WT or -ΔN, and isolation of cells with differing expression levels

To generate iMEFs stably expressing Flag-Suv39h1 WT or -ΔN, a retrovirus expression system was used. Eco-Pack 2-293 cells were transfected with pMCs-IRES-GFP carrying either Flag-Suv39h1 WT or ΔN. The obtained supernatants were then used to infect *Suv39h* DKO iMEF cells. To obtain populations expressing different levels of Suv39h1 WT or ΔN, cells were sorted by their GFP expression level, as determined by fluorescence-activated cell

sorting (FACS).

Immunofluorescence analysis

Chamber slides (#81201, ividi or #SCS-008, Matsunami) to be used for ES cells were pre-coated with 10 μg/ml of laminin for 30 min at 37°C and washed twice with PBS. Then, 2–4×10^4 ES cells or 1–2×10^4 iMEFs were plated onto the chamber slides, cultured overnight and fixed with 4% paraformaldehyde for 8 min at RT. After fixation, the cells were permeabilized with 1% Triton X-100 in PBS for 15 min at RT and incubated with 3% BSA in 0.1% Tween-20 in TBS (T-TBS) for 15 min at RT and then with primary antibodies diluted in 3% BSA in T-TBS for 1 h at RT. The cells were washed with PBS and then incubated for 1 h at RT with anti-mouse or rabbit IgG conjugated with Alexa Fluor 488, 568, or 647 as a secondary antibody, diluted in 3% BSA T-TBS and containing 1 μg/ml DAPI for nuclei counterstaining. Then, the cells were washed with PBS, mounted with in ProLong® Diamond Antifade Mountant (P36961, Thermo Fisher Scientific), and observed by confocal microscopy under an Olympus FV1000 microscope. Signal intensity of the antigen at euchromatic and pericentric DAPI-dense regions was analyzed using ImageJ.

Results

The N-terminal region of mouse Suv39h1 is essential for HP1 interaction

It has been shown that the N-terminus of Suv39h1, and Drosophila homolog Su(var)3-9, which is located upstream of the CD, interacts with the chromoshadow domain (CSD) of HP1 *in vitro* and *in vivo* (Eskeland *et al.*, 2007; Melcher *et al.*, 2000; Schotta *et al.*, 2002; Yamamoto and Sonoda, 2003). Therefore, we assayed the interaction of wild-type (WT) mouse Suv39h1 (Flag-Suv39h1 WT) and the N-terminal deletion (Δ1-41) mutant (named ΔN) with mouse HP1α, β, and γ in HEK293T cells (Fig. 1). As shown in Fig. 1B, Myc-tagged HP1α, β, and γ clearly co-immunoprecipitated with Flag-Suv39h1 WT, but not with -ΔN (center IP:Flag two panels). Anti-Myc co-immunoprecipitation experiments showed similar results (Fig. 1B, bottom IP:Myc 2 panels). This interaction partly displays the *in vivo* nature of these molecules; however, it clearly indicates that the intrinsic HP1 binding activity of Suv39h1 is lost in the ΔN mutant.

Phenotypes of Suv39h DKO ES cells expressing Flag-Suv39h1 WT and -ΔN

After confirmation that ΔN does not interact with any HP1 isoforms, we investigated how this defect impacts Suv39h1-mediated H3K9me3 formation at pericentric regions. To address this question, we introduced Flag-Suv39h1 WT or -ΔN into *Suv39h* DKO ES cells in which

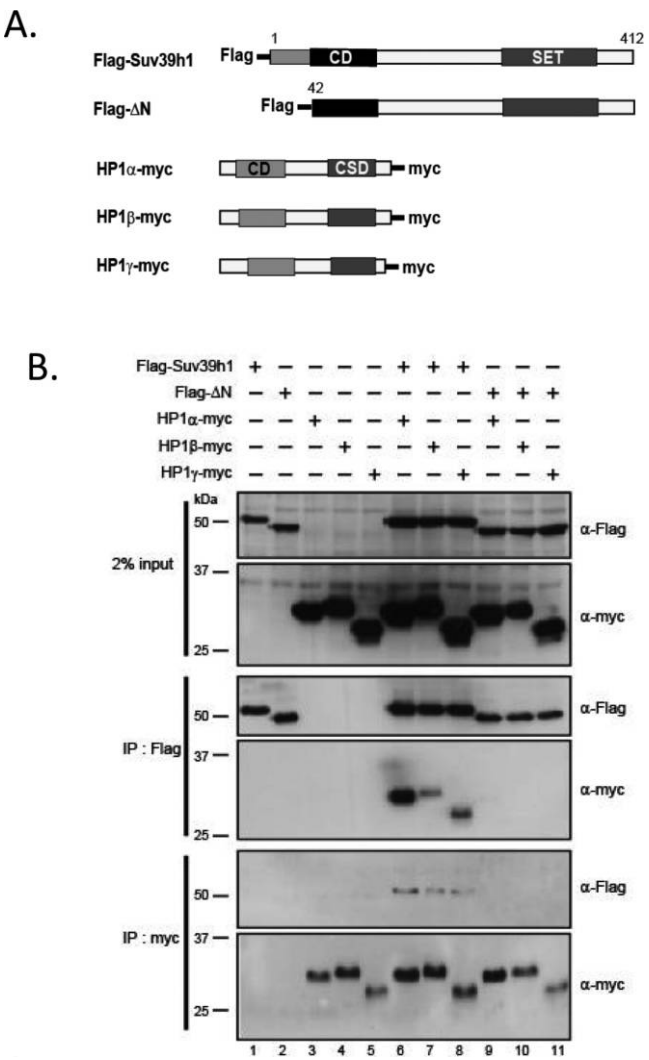

Fig. 1. Suv39h1 ΔN does not interact with HP1. A. Suv39h1 and HP1 constructs used in this study. B. Co-immunoprecipitation experiments for Suv39h1 and HP1. FLAG-Suv39h1 WT or ΔN were co-transfected with Myc-tagged HP1α, β, or γ into HEK293T cells. Forty-eight hours after transfection, extracted cell lysates were immunoprecipitated with anti-FLAG or anti-Myc antibodies and then subjected to western blot analysis with anti-FLAG or anti-Myc antibodies.

accumulation of H3K9me3 and HP1 at pericentric regions is lost. After puromycin drug selection, we examined the expression of exogenous Suv39h1 molecules in bulk or cloned transfectants by western blot analysis. As shown in Fig. 2A, bands of the expected size for Flag-Suv39h1 WT and -ΔN were detected in bulk and cloned lines, and their expression level was ~5–10 times higher than that of endogenous Suv39h1. We next examined H3K9me3 and HP1β accumulation at pericentric regions in these *Suv39h* DKO ES cells by fluorescent immunostaining (Fig. 2B and 2C). In cells expressing Flag-Suv39h1 WT, more than 90% were H3K9me3+ at the DAPI-dense pericentric regions, as

previously reported [Fig. 2B (upper panel) and 2C; (Lachner *et al.*, 2001)]. Pericentric HP1β accumulation was also mostly (~90%) restored. In contrast, *Suv39h1* DKO ES cells complemented with ΔN showed incomplete rescue with only ~20–60% becoming H3K9me3+ at the pericentric regions. Consistent with this phenotype, pericentric HP1β accumulation was observed at similar levels (Fig. 2B middle panel). However, if only the pericentric H3K9me3+ population was examined, these cells were also more than 85% HP1β+ at the pericentromeres (Fig. 2B lower panel), suggesting that HP1β can accumulate on pericentromere if H3K9me3 is enriched. We also examined heterochromatic localization of the Flag-Suv39h1 (Fig. 2D). Flag-Suv39h1 WT clearly localized to DAPI-dense regions, but Flag-ΔN foci formation on DAPI-dense regions was never detected in the bulk or cloned transgene expressing *Suv39h* DKO ES cells. Finally, we measured H3K9me3 immunofluorescence staining in euchromatin and DAPI-dense pericentric heterochromatin in *Suv39h* DKO ES cells expressing either Flag-Suv39h1 WT or -ΔN. As shown in Fig. 2C and 2E, signal intensities for the heterochromatin/euchromatin ratio were significantly higher for cells expressing Flag-Suv39h1 WT than for those expressing ΔN, indicating that H3K9me3 at pericentric regions was less abundant in cells expressing ΔN. These results indicate that the N-terminal region of Suv39h1 (amino acids 1–41) and/or HP1 interaction is crucial for efficient Suv39h1-mediated H3K9me3 establishment and/or maintenance at the pericentromeres, although it is not absolutely essential.

Phenotypes of Suv39h DKO iMEFs expressing Flag-Suv39h1 WT and -ΔN

To examine whether the findings from ES cells can be reproduced in different cell types, we performed the same experiments using *Suv39h* DKO iMEFs (Lachner *et al.*, 2001). Furthermore, we examined the relationship between the expression level of Flag-Suv39h1 WT and ΔN, and Suv39h1-mediated pericentric H3K9me3 formation. We used a retrovirus expression vector, pMCs-IRES-GFP, to infect *Suv39h* DKO iMEFs with retroviruses for Flag-Suv39h1 WT or -ΔN expression, and isolated populations with different levels of GFP marker expression (Fig. 3A). As shown in Fig. 3B, the +1 population for Flag-Suv39h1 WT showed its expression similar to that of endogenous Suv39h1. The +2 population for the same cells showed an increase in expression level of the transgene (~6x higher than that of endogenous one). In the cells infected with the retrovirus expressing ΔN, the +1, +2, +3 and +4 populations showed lower, ~3× higher, ~6× higher, and ~8× higher levels of transgene expression, respectively, than the endogenous one. Pericentric H3K9me3 and HP1β accumulation was examined 8 days post infection (Fig. 3C and 3D). Similar to *Suv39h* DKO ES cells rescued with Flag-Suv39h1 WT, more than 95% of the +1 Flag-Suv39h1 WT cells were pericentric H3K9me3+. Pericentric H3K9me3+ cells were mostly absent in the +1 and +2 populations expressing ΔN. However, in populations with increased ΔN expression, pericentric H3K9me3+ cells were significantly increased with ~40% (+3 population) and >80% (+4 population) (Fig. 3C upper panel). Pericentric HP1β accumulation was also similar to H3K9me3 accumulation (Fig. 3C middle panel). Furthermore, the majority of pericentric H3K9me3+ cells expressing ΔN were also pericentric HP1β+ (Fig. 3 lower panel). We also examined the heterochromatic localization of Flag-Suv39h1 (Fig. 3E). Flag-Suv39h1 WT clearly localized to DAPI-dense regions; however, Flag-ΔN foci formation in DAPI-dense regions was again undetectable, even at higher levels of expression (+4) in the *Suv39h* DKO iMEF cells. Signal intensities for pericentric H3K9me3 were low for ΔN-expressing cells (Fig. 3D and F). These results confirm the observations from ΔN expression in *Suv39h* DKO ES cells. Thus, ΔN's ability to establish H3K9me3 formation at the pericentromere in *Suv39h* DKO cells is severely impaired, although this can be partially overcome if ΔN is overproduced.

Discussion

In this study, we describe that ΔN is defective in establishment and/or maintenance of H3K9me3 at the pericentromere. Since ΔN is not able to bind HP1 (Fig. 1), we propose that HP1-Suv39h1 interaction is crucial for Suv39h1-mediated heterochromatin formation. However, it is still possible that another unknown function of the N-terminal region is important for this. Indeed, it was recently reported the N-terminal region of Suv39h1 (1–41) possesses chromatin-binding activity independent of its HP1 interaction (Muller *et al.*, 2016), which may also function in this process.

Although the N-terminal region of Suv39h1 was required for H3K9me3 formation at the pericentromeres and stable accumulation on them, ΔN could induce pericentric H3K9me3 if it was overproduced. This indicates that Suv39h1-mediated pericentric-specific H3K9me3 is induced by multiple signaling pathways. In yeast and plants, the RNAi pathway is crucial for establishment and maintenance of heterochromatin, including H3K9me2/3 formation (Martienssen and Moazed, 2015). Furthermore, at telomeres and mating-type regions in fission yeast, DNA-binding factors are also important for heterochromatin establishment (Jia *et al.*, 2004; Kanoh *et al.*, 2005; Kim *et al.*, 2004). Currently, involvement of the RNAi pathway in heterochromatin formation/maintenance is not clear in mammals. However, as HP1 binds RNA and nascent transcript of the major satellite repeats, this pathway is thought to have a role in HP1 recruitment to the pericentromere in mammals (Maison *et al.*, 2002; Muchardt *et al.*, 2002). Furthermore, in fission yeast, the CDs of the HP1 homolog

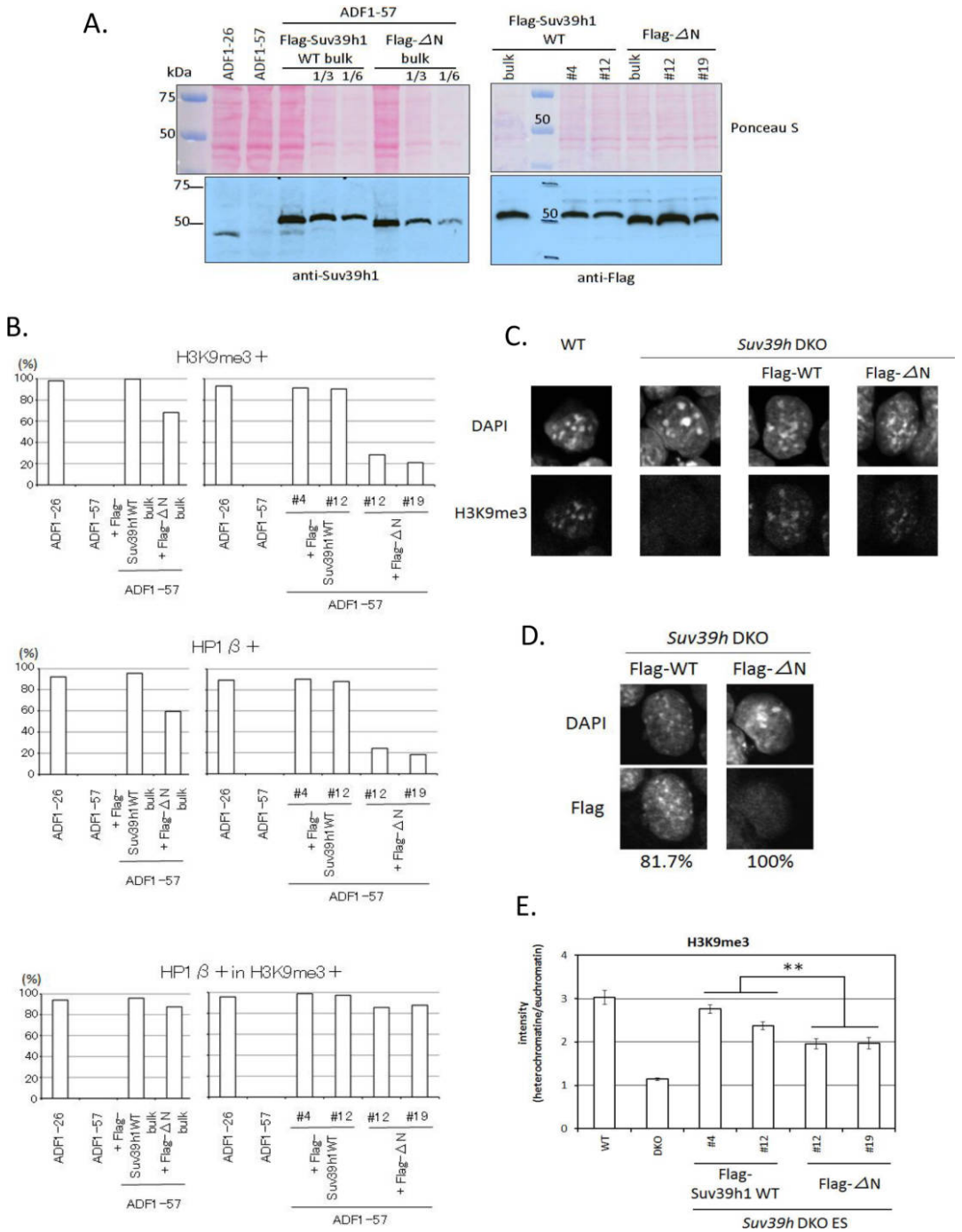

Fig. 2. Pericentric heterochromatin assembly in Suv39h DKO ES cells expressing Flag-Suv39h1 WT or ΔN. A. Western blot analysis for Suv39h1 expression in WT and Suv39h DKO ES cells with or without Flag-Suv39h1 WT or ΔN transgenes. Left panel: anti-Suv39h1, right panel: anti-Flag. ADF1-26: WT ES cells and ADF1-57: *Suv39h* DKO ES cells. B. Percentage of pericentric H3K9me3+ cells (upper), HP1β+ cells (middle) and HP1β+ cells in H3K9me3+ cells (lower). We counted more than 100 cells per sample. This is representative data from multiples repeats of the same experiment where similar phenotypes were observed. C. Representative image of a DAPI-dense pericentric H3K9me3+ cell for each indicated cell type. H3K9me3 was detected by anti-H3K9me3 ab, 2F3(Chandra *et al.*, 2012). D. Nuclear localization of Flag-Suv39h1 WT and ΔN expressed in *Suv39h* DKO ES cells. Flag-Suv39h1 WT or ΔN was detected by anti-Flag ab, M2. The number marked at the bottom of each panel indicates the percentage of cells exhibiting the phenotype. We counted more than 100 cells per sample. E. H3K9me3 signal intensity ratio between euchromatin and heterochromatin in each cell type. n≥21 sample points. (**P<0.005).

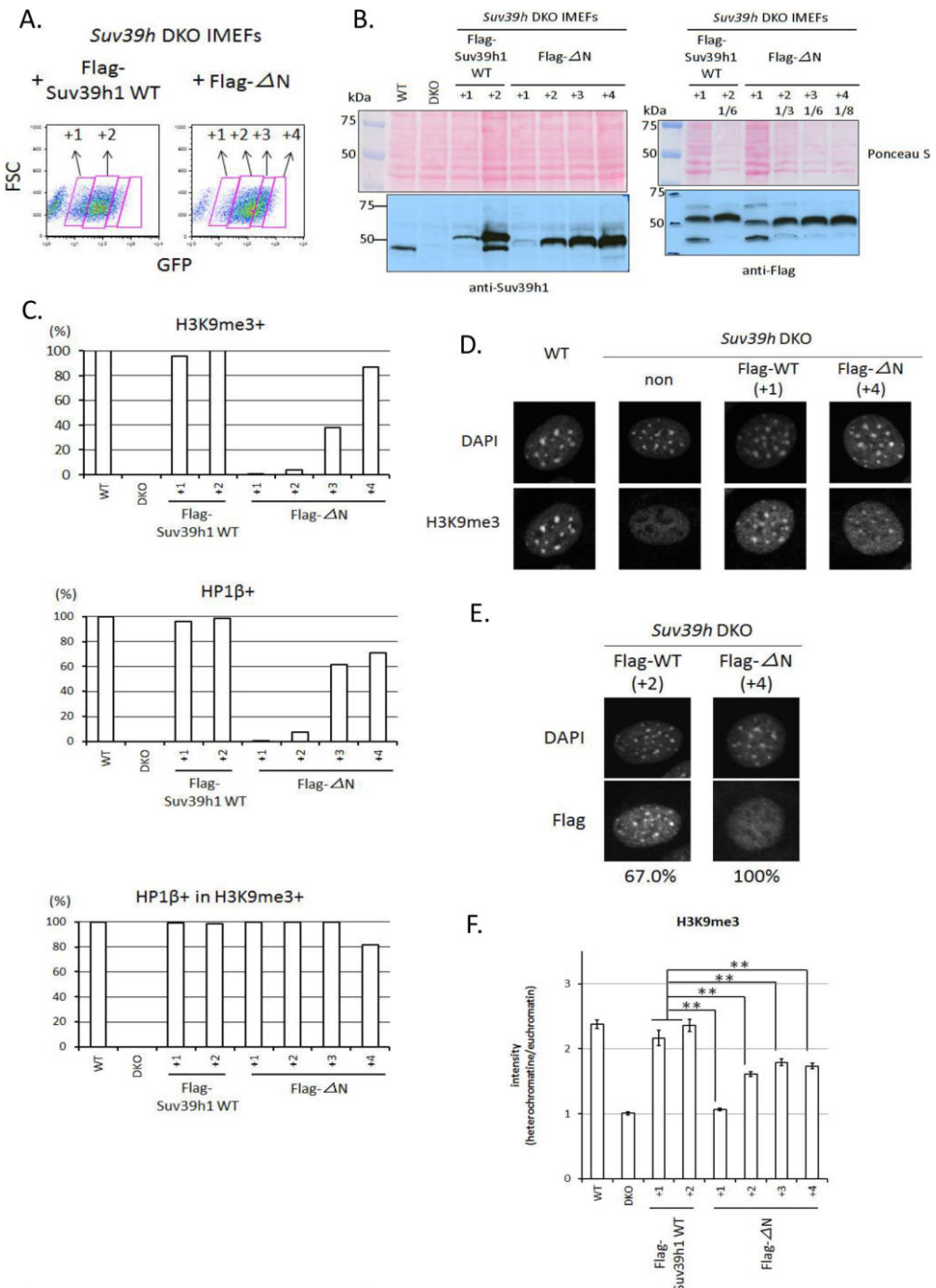

Fig. 3. Pericentric heterochromatin assembly in Suv39h DKO iMEFs expressing Flag-Suv39h1 WT or ΔN. A. Three to five days post infection, populations with different levels of GFP expression were sorted by FACS. B. Western blot analysis for Suv39h1 expression in WT and *Suv39h* DKO iMEFs infected with or without the retrovirus for Flag-Suv39h1 WT or ΔN. Left panel: anti-Suv39h1, right panel: anti-Flag. +1~+4 are shown in A. C. Percentages of pericentric H3K9me3+ cells (upper), HP1β+ cells (middle) and HP1β+ cells in H3K9me3+ cells (lower). We counted more than 100 cells per sample. This is representative data from multiple repeats of the same experiment where similar phenotypes were observed. D. Representative image of a DAPI-dense pericentric H3K9me3+ cell for each indicated cell type. H3K9me3 was detected by anti-H3K9me3 ab, 2F3. E. Nuclear localization of Flag-Suv39h1 WT and ΔN expressed in *Suv39h* DKO iMEF cells. Flag-Suv39h1 WT or ΔN was detected by anti-Flag ab, M2. The number marked at the bottom of each panel indicates percentage of the cells showing the phenotype. We counted more than 100 cells per sample. F. H3K9me3 signal intensity ratio between euchromatin and heterochromatin in each cell type. n≥26 sample points. (**P<0.005).

Chp1, and the Suv39h homolog Clr4, possess RNA-binding activity that is linked to heterochromatin assembly (Ishida *et al.*, 2012). Therefore, it is possible that Suv39h1 also possesses RNA-binding activity, and nascent transcript is involved in creating Suv39h1's target specificity. In addition, it is already known that Suv39h1 CD possesses higher binding affinities for H3K9me2/3 (Wang *et al.*, 2012). In *Suv39h* DKO cells, pericentric H3K9me3 is severely diminished, but global H3K9me3 is still heavily maintained by other H3K9 methyltransferases (Bulut-Karslioglu *et al.*, 2014). If residual H3K9me3 catalyzed by other enzymes is present in the pericentric regions of *Suv39h* DKO cells, it makes possible to recruit residual amount of HP1 and Suv39h1 to the pericentromere. This phenomenon might also have a role in the ΔN-mediated pericentric H3K9me3 formation. DNA-binding transcription factors has also been shown to be involved in heterochromatin formation in mammals (Bulut-Karslioglu *et al.*, 2012). These factors may interact with Suv39h1 through domains other than the N-terminal region and recruit it to the pericentromeres. Our new findings provide insights to understand how heterochromatin assembly is initiated and maintained at specific loci in mammals.

Acknowledgments. We thank Dr. Thomas Jenuwein for providing *Suv39h* DKO ES and iMEF cell lines, Dr. Hitoshi Niwa for providing pPBCAGGS-IRESpuro and pCAGGS-PBase vectors, Drs. Chikashi Obuse and Ryo-suke Nozawa for technical advice on HP1 immunoprecipitation experiments, and all members of the Shinkai lab, especially Dr. Masaki Kato, for their experimental support, critical feedback, and suggestions. This work was supported in part by a grant-in-aid from the Ministry of Education, Culture, Sports, Science and Technology of Japan and by AMED-CREST.

References

Allis, C.D., Jenuwein, T., Reinberg, D., and Caparros, M.L. 2007. Overview and concepts. In: Epigenetics (C.D. Allis, T. Jenuwein, D. Reinberg, and M.L. Caparros, eds.). Cold Spring Harbor Laboratory Press, pp. 23–61.

Allshire, R.C. and Karpen, G.H. 2008. Epigenetic regulation of centromeric chromatin: old dogs, new tricks? *Nat. Rev. Genet.*, **9**: 923–937.

Bannister, A.J., Zegerman, P., Partridge, J.F., Miska, E.A., Thomas, J.O., Allshire, R.C., and Kouzarides, T. 2001. Selective recognition of methylated lysine 9 on histone H3 by the HP1 chromo domain. *Nature*, **410**: 120–124.

Black, J.C. and Whetstine, J.R. 2011. Chromatin landscape: methylation beyond transcription. *Epigenetics*, **6**: 9–15.

Bulut-Karslioglu, A., Perrera, V., Scaranaro, M., de la Rosa-Velazquez, I.A., van de Nobelen, S., Shukeir, N., Popow, J., Gerle, B., Opravil, S., Pagani, M., *et al.* 2012. A transcription factor-based mechanism for mouse heterochromatin formation. *Nat. Struct. Mol. Biol.*, **19**: 1023–1030.

Bulut-Karslioglu, A., De La Rosa-Velazquez, I.A., Ramirez, F., Barenboim, M., Onishi-Seebacher, M., Arand, J., Galan, C., Winter, G.E., Engist, B., Gerle, B., *et al.* 2014. Suv39h-dependent H3K9me3 marks intact retrotransposons and silences LINE elements in mouse embryonic stem cells. *Mol. Cell*, **55**: 277–290.

Chandra, T., Kirschner, K., Thuret, J.Y., Pope, B.D., Ryba, T., Newman, S., Ahmed, K., Samarajiwa, S.A., Salama, R., Carroll, T., *et al.* 2012. Independence of repressive histone marks and chromatin compaction during senescent heterochromatic layer formation. *Mol. Cell*, **47**: 203–214.

Eissenberg, J.C., James, T.C., Foster-Hartnett, D.M., Hartnett, T., Ngan, V., and Elgin, S.C. 1990. Mutation in a heterochromatin-specific chromosomal protein is associated with suppression of position-effect variegation in Drosophila melanogaster. *Proc. Natl. Acad. Sci. USA*, **87**: 9923–9927.

Eskeland, R., Eberharter, A., and Imhof, A. 2007. HP1 binding to chromatin methylated at H3K9 is enhanced by auxiliary factors. *Mol. Cell. Biol.*, **27**: 453–465.

Grewal, S.I. and Elgin, S.C. 2002. Heterochromatin: new possibilities for the inheritance of structure. *Curr. Opin. Genet. Dev.*, **12**: 178–187.

Hall, I.M., Shankaranarayana, G.D., Noma, K., Ayoub, N., Cohen, A., and Grewal, S.I. 2002. Establishment and maintenance of a heterochromatin domain. *Science*, **297**: 2232–2237.

Ishida, M., Shimojo, H., Hayashi, A., Kawaguchi, R., Ohtani, Y., Uegaki, K., Nishimura, Y., and Nakayama, J. 2012. Intrinsic nucleic acid-binding activity of Chp1 chromodomain is required for heterochromatic gene silencing. *Mol. Cell*, **47**: 228–241.

Jia, S., Noma, K., and Grewal, S.I. 2004. RNAi-independent heterochromatin nucleation by the stress-activated ATF/CREB family proteins. *Science*, **304**: 1971–1976.

Kanoh, J., Sadaie, M., Urano, T., and Ishikawa, F. 2005. Telomere binding protein Taz1 establishes Swi6 heterochromatin independently of RNAi at telomeres. *Curr. Biol.*, **15**: 1808–1819.

Kim, H.S., Choi, E.S., Shin, J.A., Jang, Y.K., and Park, S.D. 2004. Regulation of Swi6/HP1-dependent heterochromatin assembly by cooperation of components of the mitogen-activated protein kinase pathway and a histone deacetylase Clr6. *J. Biol. Chem.*, **279**: 42850–42859.

Kouzarides, T. and Berger, S.L. 2007. Chromatin modifications and their mechanism of action. In: Epigenetics (C.D. Allis, T. Jenuwein, D. Reinberg, and M.L. Caparros, eds.). Cold Spring Harbor Laboratory Press, pp. 191–209.

Lachner, M., O'Carroll, D., Rea, S., Mechtler, K., and Jenuwein, T. 2001. Methylation of histone H3 lysine 9 creates a binding site for HP1 proteins. *Nature*, **410**: 116–120.

Lehnertz, B., Ueda, Y., Derijck, A.A., Braunschweig, U., Perez-Burgos, L., Kubicek, S., Chen, T., Li, E., Jenuwein, T., and Peters, A.H. 2003. Suv39h-mediated histone H3 lysine 9 methylation directs DNA methylation to major satellite repeats at pericentric heterochromatin. *Curr. Biol.*, **13**: 1192–1200.

Maison, C., Bailly, D., Peters, A.H., Quivy, J.P., Roche, D., Taddei, A., Lachner, M., Jenuwein, T., and Almouzni, G. 2002. Higher-order structure in pericentric heterochromatin involves a distinct pattern of histone modification and an RNA component. *Nat. Genet.*, **30**: 329–334.

Martienssen, R. and Moazed, D. 2015. RNAi and heterochromatin assembly. Cold Spring Harbor Perspectives in Biology, *7*, a019323.

Melcher, M., Schmid, M., Aagaard, L., Selenko, P., Laible, G., and Jenuwein, T. 2000. Structure-function analysis of SUV39H1 reveals a dominant role in heterochromatin organization, chromosome segregation, and mitotic progression. *Mol. Cell. Biol.*, **20**: 3728–3741.

Muchardt, C., Guilleme, M., Seeler, J.S., Trouche, D., Dejean, A., and Yaniv, M. 2002. Coordinated methyl and RNA binding is required for heterochromatin localization of mammalian HP1alpha. *EMBO Rep.*, **3**: 975–981.

Muller, M.M., Fierz, B., Bittova, L., Liszczak, G., and Muir, T.W. 2016. A two-state activation mechanism controls the histone methyltransferase Suv39h1. *Nat. Chem. Biol.*, **12**: 188–193.

Ohtsuka, S., Nishikawa-Torikai, S., and Niwa, H. 2012. E-cadherin promotes incorporation of mouse epiblast stem cells into normal development. *PloS one*, **7**: e45220.

Schotta, G., Ebert, A., Krauss, V., Fischer, A., Hoffmann, J., Rea, S.,

Jenuwein, T., Dorn, R., and Reuter, G. 2002. Central role of Drosophila SU(VAR)3-9 in histone H3-K9 methylation and heterochromatic gene silencing. *The EMBO J.*, **21**: 1121–1131.

Schotta, G., Lachner, M., Sarma, K., Ebert, A., Sengupta, R., Reuter, G., Reinberg, D., and Jenuwein, T. 2004. A silencing pathway to induce H3-K9 and H4-K20 trimethylation at constitutive heterochromatin. *Gene. Dev.*, **18**: 1251–1262.

Taverna, S.D., Li, H., Ruthenburg, A.J., Allis, C.D., and Patel, D.J. 2007. How chromatin-binding modules interpret histone modifications: lessons from professional pocket pickers. *Nat. Struct. Mol. Biol.*, **14**: 1025–1040.

Vissel, B. and Choo, K.H. 1989. Mouse major (gamma) satellite DNA is highly conserved and organized into extremely long tandem arrays: implications for recombination between nonhomologous chromosomes. *Genomics*, **5**: 407–414.

Wang, T., Xu, C., Liu, Y., Fan, K., Li, Z., Sun, X., Ouyang, H., Zhang, X., Zhang, J., Li, Y., *et al.* 2012. Crystal Structure of the Human SUV39H1 Chromodomain and Its Recognition of Histone H3K9me2/3. *PloS one*, **7**: e52977.

Yamamoto, K. and Sonoda, M. 2003. Self-interaction of heterochromatin protein 1 is required for direct binding to histone methyltransferase, SUV39H1. *Biochem. Biophys. Res. Commun.*, **301**: 287–292.

Zeng, W., Ball, A.R., Jr., and Yokomori, K. 2010. HP1: heterochromatin binding proteins working the genome. *Epigenetics*, **5**: 287–292.

(Received for publication, July 30, 2016, accepted, October 4, 2016 and published online, October 12, 2016)